Current Optics and Photonics
Vol. 3, No. 4, August 2019, pp. 311-319

ISSN: 2508-7266(Print) / ISSN: 2508-7274(Online)
DOI: https://doi.org/10.3807/COPP.2019.3.4.311

Performance Analysis of an AF Dual-hop FSO Communication System with RF Backup Link

Khaled A. Alhamawi[1,2] and Essam S. Altubaishi[2]*

[1]*Huawei Technologies, C-Center Tahlia Road, Riyadh 1135, Saudi Arabia*
[2]*Department of Electrical Engineering, King Saud University, Riyadh 11421, Saudi Arabia*

(Received February 13, 2019 : revised May 12, 2019 : accepted May 14, 2019)

A hybrid free-space-optical/radio-frequency (FSO/RF) communication system is considered, with the help of amplify-and-forward (AF) relaying. We consider various weather conditions to investigate their effects on the system's performance. We begin by obtaining the cumulative distribution function and probability density function of the end-to-end signal-to-noise ratio for the AF dual-hop FSO communication system with RF backup link. Then, these results are used to derive closed-form expressions for the outage probability, average bit-error rate, and average ergodic capacity. The results show that the considered system efficiently employs the complementary nature of FSO and RF links, resulting in impressive performance improvements compared to non-hybrid systems.

Keywords : Free space optical communication, Hybrid FSO/RF communication, Outage probability, bit-error rate, Ergodic capacity
OCIS codes : (010.1330) Atmospheric turbulence; (010.3310) Laser beam transmission; (060.2605) Free-space optical communication

I. INTRODUCTION

Recently, free-space optical (FSO) communication has been considered a promising alternative solution to conventional transmission techniques, such as fiber optics and RF transmission. This is due to its ability to provide high data rates, high optical bandwidth, and use of the license-free spectrum. Despite these advantages, the performance of an FSO link depends greatly on weather conditions, such as fog, rain, snow, haze, and dust, which may limit performance and reliability. Another major impairment is the fading induced by atmospheric turbulence, which causes irradiance fluctuations in the received optical signal, and leads to poor performance.

The performance of an FSO link under various effects or conditions was studied in [1-8]. In [3] and [4], the atmospheric turbulence was modeled as a log-normal distribution, where the FSO link was evaluated under the effect of irreducible error floors caused by using demodulation with fixed detection thresholds. A similar turbulence model was used in [5] to study the performance of retroreflector free-space optical systems. [6] and [7] proposed two techniques to improve the performance of FSO links under log-normal turbulence by exploiting source-information transformation and spatial diversity. In [8], the probabilistic behavior of an FSO channel in fog was investigated, and a new statistical model for signal attenuation developed.

Relay-assisted transmission has also been proposed to mitigate weather conditions and turbulence-induced fading. In [9], an FSO communication system with amplify-and-forward (AF) relaying was investigated over log-normal turbulence channels, in terms of outage probability. The results showed a significant gain improvement over direct transmission. In [10], the performance of a two-way relay-assisted FSO communication system over atmospheric-turbulence-induced fading channels was considered. In [11], a dual-hop AF mixed FSO/RF transmission system was investigated, assuming a gamma-gamma distribution for the

*Corresponding author: etubashi@ksu.edu.sa, ORCID 0000-0003-1422-8383
Color versions of one or more of the figures in this paper are available online.

FSO link and an distribution for the RF link. Later, [12] extended the work of [11] by assuming a Rician distribution for the RF link and a Malaga distribution for the FSO link. In [13], a triple-hop multiuser mixed RF/FSO/RF communication system was studied, where the first and third RF links were modeled as a Rayleigh distribution, while the second FSO link was modeled as a gamma-gamma distribution.

The combination of FSO and RF transmissions is another technique for enhancing FSO performance, where the two links can operate in a complementary manner. In [14], a hybrid FSO/RF communication system was investigated, assuming that the system switches between direct FSO and RF links using a predefined threshold. To avoid frequent on/off transitions of the FSO link, dual FSO thresholds were proposed in [15]. Numerical results showed that dual FSO thresholds achieve a similar performance to that of the single FSO threshold. Another hybrid FSO/RF communication system was proposed in [16], assuming that the receiver receives the same information from the two links; thus selective combining (SC) or maximal-ratio combining (MRC) is used. The results illustrated that MRC provides better performance than SC does. From another perspective, a hybrid FSO/RF communication system with adaptive combining was presented in [17], where the RF link is activated under the condition that the FSO link's quality is low, in which MRC is used to combine the received signals from both FSO and RF links. The results indicated that the considered system outperforms an FSO-only or RF-only setup. In [18], the outage probability was investigated for different multihop hybrid FSO/RF scenarios, considering log-normal turbulence and various weather conditions.

In this paper, we aim to improve the performance of the FSO system against path loss and atmospheric turbulence (1) by exploiting relay-assisted transmission, not only as an efficient technique to reduce the turbulence effect, but also to ensure the line-of-site requirement in FSO transmission; and (2) by employing an RF backup link, to improve transmission reliability when FSO links experience an outage. Specifically, a dual-hop FSO transmission is used if the target quality is achieved, else the system will activate the RF link. We consider a channel model with both path loss and atmospheric turbulence, modeled by a log-normal distribution for the FSO links and a Rayleigh distribution for the RF backup link. Furthermore, we investigate the effects of weather on the performance of the considered system for the most common deterrent conditions, fog and rain, and compare it to a dual-hop FSO system. Mathematical expressions for the probability density function (PDF) and cumulative distribution function (CDF) for the end-to-end signal-to-noise ratio (SNR) are obtained. Then, closed-form expressions for the outage probability, average BER, and average ergodic capacity are derived. We believe that the derivation of PDF and CDF of the end-to-end SNR will help researchers in optical communication, either in the physical or upper layers, to evaluate the system further from a different angle, or to modify the system to introduce a new scheme. Furthermore, the derived expressions for the performance metrics as functions of path loss and weather conditions will provide an additional evaluation of the system by changing, for instance, the distance, or the weather-condition parameter.

The remainder of the paper is organized as follows: The system and channel models are presented in section II. Statistical characteristics, including the end-to-end PDF and CDF of the considered dual-hop FSO system with RF backup link, are provided in section III. Based on these expressions, closed-form expressions for the outage probability, average BER, and average ergodic capacity are derived in section IV. Numerical results are discussed in section V. Finally, the paper is concluded in section VI.

II. SYSTEM AND CHANNEL MODELS

In this work, we consider a dual-hop FSO communication system using the AF relaying protocol and supported by an RF backup link, as shown in Fig. 1. The dual-hop FSO link is the primary link for transmission, which is used if its SNR γ_{FSO} is larger than a predefined threshold $\gamma_{FSO,th}$. Otherwise the RF link is activated, if its SNR γ_{RF} is larger than a certain threshold $\gamma_{RF,th}$ as well. If both links are below both thresholds, the system is under outage.

2.1. Dual-hop FSO Link

The FSO link is assumed to employ binary phase-shift keying (BPSK) subcarrier intensity modulation (SIM) [19]. The electrical subcarrier signal $m(t)$ is DC biased to become non-negative. Then the transmitted signal from source to relay can be given as

$$x_S = P_S(1+\mu_S m(t)) \tag{1}$$

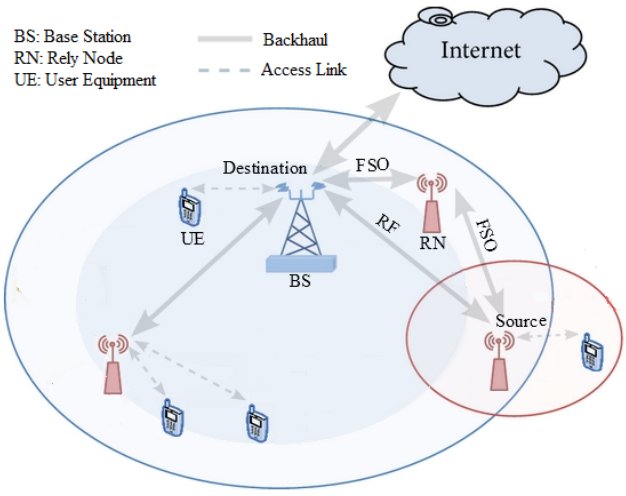

FIG. 1. AF Dual-hop FSO communication system with backup RF link.

where P_S is the average transmitted optical power, and $\mu_S(0 < \mu_S < 1)$ is the modulation index, used to avoid over modulation-induced clipping. The received signal at the relay node can be written as

$$x_R = h_1 x_S + n_1 \tag{2}$$

where n_1 is additive white Gaussian noise (AWGN) with zero mean and variance $\sigma_1^2 = \mathrm{E}[|n_1|^2]$, where E[.] represents the mathematical expectation operation. $h_1 = h_{pl_1} h_{at_1}$ is the fading coefficient of the source-relay link, which consists of path loss h_{pl_1}, and atmospheric turbulence h_{at_1}. The received signal at the relay node is then amplified and forwarded to the destination node. The received signal at the destination node can be written as

$$\begin{aligned} x_D &= G h_2 x_R + n_2 \\ &= G h_1 h_2 P_S \left(1 + \mu_S m(t)\right) + G h_2 n_1 + n_2 \end{aligned} \tag{3}$$

where n_2 represents AWGN with zero mean and variance $\sigma_2^2 = \mathrm{E}[|n_2|^2]$, and $h_2 = h_{pl_2} h_{at_2}$ is the fading coefficient of the relay-destination link, which is a function of the path loss h_{pl_2} and the atmospheric turbulence h_{at_2}. G represents the relay gain, given by

$$G = \sqrt{\frac{P_R}{h_1^2 P_S^2 \mu_S^2 + \sigma_1^2}} \tag{4}$$

where P_R is the average transmitted optical power of the relay node. The received signal, after blocking the DC signal in Eq. (3), becomes

$$x_D = G h_1 h_2 P_S \mu_S m(t) + G h_2 n_1 + n_2 \tag{5}$$

2.1.1. Channel path loss

The path loss of the optical signal along the atmospheric channel can be given by the Beers-Lambert law [20] as

$$h_{pl_i} = \exp(-\alpha_i L_i), \qquad i = 1, 2 \tag{6}$$

where h_{pl_i} denotes the path loss for the i^{th} hop, L_i is the distance of the FSO link (in km), and α_i is the attenuation coefficient (in km^{-1}), which depends on the weather conditions, such as fog and haze, and which can be calculated as [21]

$$\alpha_i = \frac{3.912}{V}\left(\frac{\lambda}{550}\right)^{-\varepsilon} \tag{7}$$

where V is the visibility range (in km), λ is the operating wavelength (in nm), and ε is a parameter related to the visibility, given by the Kruse model as 1.6 if $V > 50$ km, 1.3 if $6 < V < 50$ km, and $0.585V^{1/3}$ if $V < 6$ km [22]. For rainy weather conditions, α_i is given by $\alpha_i = 1.076 R_{rain}^{0.67}$ (dB/km), where R_{rain} denotes the rain rate (in mm/h) [23].

2.1.2. Turbulence statistical model

We consider atmospheric turbulence in which the intensity fluctuation's PDF is modeled using a log-normal distribution. Let the channel's fading amplitude $h_{at_i} = \exp(2x_i)$ follow a log-normal distribution with PDF expressed as [24]

$$f_{h_{at_i}}(h) = \frac{1}{\sqrt{8\pi\sigma_{x_i}^2}\, h} \exp\left(\frac{-\left(\ln(h) - 2\mu_{x_i}\right)^2}{8\sigma_{x_i}^2}\right) \tag{8}$$

where x_i represents a Gaussian-distributed random variable with mean μ_{x_i} and variance $\sigma_{x_i}^2$. To make sure the average power is not attenuated or amplified due to fading, the amplitude of fading needs to be normalized as $\mathrm{E}[h_{at_i}] = 1$. This implies $\mu_{x_i} = -\sigma_{x_i}^2$. In this case, Eq. (8) can be rewritten as

$$f_{h_{at_i}}(h) = \frac{1}{\sqrt{8\pi\sigma_{x_i}^2}\, h} \exp\left(\frac{-\left(\ln(h) + 2\sigma_{x_i}^2\right)^2}{8\sigma_{x_i}^2}\right) \tag{9}$$

where the variance $\sigma_{x_i}^2$ is given by [25]

$$\sigma_{x_i}^2 = 0.307 k^{7/6} L_i^{11/6} C_{n_i}^2 \tag{10}$$

where $k = 2\pi/\lambda$ is the optical wave number, and $C_{n_i}^2$ is the index of refraction structure parameter.

2.1.3. SNR statistics

Based on Eq. (5), the dual-hop FSO link's SNR can be written as

$$\gamma_{FSO} = \frac{h_1^2 G^2 P_S^2 \mu_S^2 h_2^2}{h_2^2 G^2 \sigma_1^2 + \sigma_2^2} = \frac{\gamma_1 \gamma_2}{\gamma_1 + \gamma_2 + 1} \tag{11}$$

where $\gamma_1 = P_S^2 \mu_S^2 h_1^2 / \sigma_1^2 = \bar{\gamma}_1 h_{at_1}^2$ and $\gamma_2 = P_R h_2^2 / \sigma_2^2 = \bar{\gamma}_2 h_{at_2}^2$ are the per-hop SNRs, $\bar{\gamma}_1 = P_S^2 \mu_S^2 h_{pl_1}^2 / \sigma_1^2$ and $\bar{\gamma}_2 = P_R h_{pl_2}^2 / \sigma_2^2$ are the average SNRs for the 1st and 2nd hops respectively. For the simplicity of derivation, Eq. (11) can be approximated by its upper bound [26]

$$\gamma_{FSO} \le \min(\gamma_1, \gamma_2) \tag{12}$$

Based on Eq. (9) and Eq. (2.3) of [27], the PDF of γ_i can be expressed as

$$f_{\gamma_i}(\gamma)=\frac{1}{\sqrt{32\pi\sigma_{x_i}^2}\,\gamma}\exp\left(\frac{-\left(\ln(\frac{\gamma}{\overline{\gamma}_i})+4\sigma_{x_i}^2\right)^2}{32\sigma_{x_i}^2}\right) \quad (13)$$

Integrating Eq. (13) with respect to γ, the corresponding CDF can be obtained as

$$F_{\gamma_i}(\gamma)=1-\frac{1}{2}\mathrm{erfc}\left(\frac{\ln(\frac{\gamma}{\overline{\gamma}_i})+4\sigma_{x_i}^2}{\sqrt{32}\sigma_{x_i}}\right) \quad (14)$$

2.2. RF Backup Link

For the RF link (*i.e.* source-destination link), the BPSK-modulated signal is up-converted using a 60-GHz carrier. The received signal at the destination is given by

$$x_D = h_{RF}x_{RF}+n_{RF}, \quad (15)$$

where x_{RF} represents the transmitted symbol with average power of $\mathrm{E}[|x_{RF}|^2]=P_{RF}$, n_{RF} is AWGN with zero mean and variance $\sigma_{RF}^2=\mathrm{E}[|n_{RF}|^2]$, and h_{RF} is the RF channel's gain, factorized as $h_{RF}=\sqrt{h_{pl_{RF}}}h_f$. Here $h_{pl_{RF}}$ denotes the RF channel's path loss, and h_f represents the fading coefficient. The noise variance of the RF link is given by [16] as $\sigma_{RF}^2=B_{RF}+N_o+N_F$, where B_{RF} is the bandwidth, N_o is the noise's power spectral density, and N_F is the receiver's noise figure.

2.2.1. Channel path loss

The path loss of the RF channel is given as [18]

$$h_{pl_{RF}}=G_t+G_r-20\log_{10}\left(\frac{4\pi L}{\lambda_{RF}}\right)-\alpha_{oxy}L-\alpha_{rain}L \quad (16)$$

where G_t and G_r denote the gains of transmitter and receiver respectively, L is the distance between source and destination, λ_{RF} is the RF wavelength, and α_{oxy} and α_{rain} represent the attenuation factors due to absorption and rain scattering respectively.

2.2.2. Fading statistical model

In this paper, we consider the Rayleigh fading model for the RF channel, where the PDF can be given by [27]

$$f_{h_f}(h)=\frac{2h}{\sigma_s^2}e^{\frac{-h^2}{\sigma_s^2}} \quad (17)$$

where σ_s is the root mean square of the received signal.

2.2.3. SNR statistics

Based on Eq. (15), the RF link's SNR can be written as

$$\gamma_{RF}=\frac{P_{RF}h_{RF}^2}{\sigma_{RF}^2}=\overline{\gamma}_{RF}h_f^2 \quad (18)$$

where $\overline{\gamma}_{RF}=P_{RF}h_{pl_{RF}}/\sigma_{RF}^2$ is the average SNR. The PDF of γ_{RF} can be written as

$$f_{\gamma_{RF}}(\gamma)=\frac{1}{\overline{\gamma}_{RF}}e^{\frac{-\gamma}{\overline{\gamma}_{RF}}} \quad (19)$$

and its CDF can be obtained as

$$F_{\gamma_{RF}}(\gamma)=1-e^{\frac{-\gamma}{\overline{\gamma}_{RF}}} \quad (20)$$

III. END-TO-END STATISTICAL CHARACTERISTICS

In this section, the CDF and PDF of the end-to-end SNR of the AF dual-hop FSO system with RF backup link are obtained.

3.1. Cumulative Distribution Function

For a dual-hop FSO link using AF relaying, the CDF of the received SNR can be defined as

$$F_{\gamma_{FSO}}(\gamma)=1-(1-F_{\gamma_1}(\gamma))(1-F_{\gamma_2}(\gamma)) \quad (21)$$

where $F_{\gamma_1}(\gamma)$ and $F_{\gamma_2}(\gamma)$ are the CDFs of the 1st and the 2nd FSO hops respectively. Substituting Eq. (14) into Eq. (21), $F_{\gamma_{FSO}}(\gamma)$ becomes

$$F_{\gamma_{FSO}}(\gamma)=1-\frac{1}{4}\mathrm{erfc}\left(\frac{\ln(\frac{\gamma}{\overline{\gamma}_1})+4\sigma_{x_1}^2}{\sqrt{32}\sigma_{x_1}}\right)\mathrm{erfc}\left(\frac{\ln(\frac{\gamma}{\overline{\gamma}_2})+4\sigma_{x_2}^2}{\sqrt{32}\sigma_{x_2}}\right) \quad (22)$$

The CDF of the end-to-end SNR can be defined as

$$F_{e2e}(\gamma)=F_{\gamma_{FSO}}(\gamma)F_{\gamma_{RF}}(\gamma) \quad (23)$$

Substituting Eqs. (20) and (22) into Eq. (23), a closed-form expression for $F_{e2e}(\gamma)$ can be obtained.

3.2. Probability Density Function

The PDF of the SNR of the AF dual-hop FSO system can be found by differentiating Eq. (21) with respect to γ, that is

$$f_{\gamma_{FSO}}(\gamma) = f_{\gamma_1}(\gamma) + f_{\gamma_2}(\gamma) - f_{\gamma_1}(\gamma)F_{\gamma_2}(\gamma) - F_{\gamma_1}(\gamma)f_{\gamma_2}(\gamma) \quad (24)$$

where $f_{\gamma_1}(\gamma)$ and $f_{\gamma_2}(\gamma)$ are the PDFs of the 1st and 2nd FSO links respectively. Substituting Eqs. (13) and (14) into Eq. (24), $f_{\gamma_{FSO}}(\gamma)$ becomes

$$f_{\gamma_{FSO}}(\gamma) = \frac{1}{2\sqrt{32\pi\gamma}}\left\{\frac{1}{\sigma_1}\exp\left(\frac{-\left(\ln(\frac{\gamma}{\bar{\gamma}_1})+4\sigma_1^2\right)^2}{32\sigma_1^2}\right)\operatorname{erfc}\left(\frac{\ln(\frac{\gamma}{\bar{\gamma}_2})+4\sigma_2^2}{\sqrt{32}\sigma_2}\right) + \frac{1}{\sigma_2}\exp\left(\frac{-\left(\ln(\frac{\gamma}{\bar{\gamma}_2})+4\sigma_2^2\right)^2}{32\sigma_2^2}\right)\operatorname{erfc}\left(\frac{\ln(\frac{\gamma}{\bar{\gamma}_1})+4\sigma_1^2}{\sqrt{32}\sigma_1}\right)\right\} \quad (25)$$

The PDF of the end-to-end SNR can be also found by differentiating Eq. (23) with respect to γ, which can be given as

$$f_{e2e}(\gamma) = f_{\gamma_{FSO}}(\gamma)F_{\gamma_{RF}}(\gamma) + F_{\gamma_{FSO}}(\gamma)f_{\gamma_{RF}}(\gamma) \quad (26)$$

$f_{e2e}(\gamma)$ can be obtained by substituting Eqs. (19), (20), (22), and (25) into Eq. (26).

IV. PERFORMANCE ANALYSIS

In this section we derive closed-form analytical expressions for the outage probability, average BER, and ergodic capacity, based on the expressions derived in the previous section.

4.1. Outage Probability

The outage probability of the considered system is defined as the probability that the instantaneous SNRs γ_{FSO} and γ_{RF} both fall below their respective thresholds $\gamma_{FSO,th}$ and $\gamma_{RF,th}$. Setting $\gamma = \gamma_{RF,th}$ in Eq. (20) and $\gamma = \gamma_{FSO,th}$ in Eq. (22), and assuming that the FSO links are symmetric (*i.e.* $\bar{\gamma}_1 = \bar{\gamma}_2 = \bar{\gamma}$ and $\sigma_{x_1} = \sigma_{x_2} = \sigma$), the outage probability can be obtained as

$$OP = F_{\gamma_{FSO}}(\gamma_{FSO,th})F_{\gamma_{RF}}(\gamma_{RF,th}) = \left[1 - \frac{1}{4}\operatorname{erfc}^2\left(\frac{\ln(\frac{\gamma_{FSO,th}}{\bar{\gamma}})+4\sigma^2}{\sqrt{32}\sigma}\right)\right]\left(1 - e^{\frac{-\gamma_{RF,th}}{\bar{\gamma}_{RF}}}\right) \quad (27)$$

4.2. Average BER

The average BER of the considered system can be expressed as

$$BER = \frac{ber_{\gamma_{FSO,th}} + F_{\gamma_{FSO}}(\gamma_{FSO,th})ber_{\gamma_{RF,th}}}{1 - OP} \quad (28)$$

where $ber_{\gamma_{FSO,th}}$ and $ber_{\gamma_{RF,th}}$ are given by

$$ber_{\gamma_{FSO,th}} = \int_{\gamma_{FSO,th}}^{\infty} P(e \mid \gamma) f_{\gamma_{FSO}}(\gamma)\, d\gamma \quad (29)$$

and

$$ber_{\gamma_{RF,th}} = \int_{\gamma_{RF,th}}^{\infty} P(e \mid \gamma) f_{\gamma_{RF}}(\gamma)\, d\gamma \quad (30)$$

where $P(e \mid \gamma)$ is the BER of the AWGN channel, which for the case of BPSK modulation can be given as $P(e \mid \gamma) = 0.5\operatorname{erfc}(\sqrt{\gamma})$ [27]. For symmetrical FSO links, $ber_{\gamma_{FSO,th}}$ can be obtained by substituting Eq. (25) into Eq. (29) as

$$ber_{\gamma_{FSO,th}} = \int_{\gamma_{FSO,th}}^{\infty} \frac{\operatorname{erfc}(\sqrt{\gamma})}{2\sqrt{32\pi\gamma}\sigma}\exp\left(\frac{-\left(\ln(\frac{\gamma}{\bar{\gamma}})+4\sigma^2\right)^2}{32\sigma^2}\right)\operatorname{erfc}\left(\frac{\ln(\frac{\gamma}{\bar{\gamma}})+4\sigma^2}{\sqrt{32}\sigma}\right) d\gamma \quad (31)$$

Using the erfc function's series expansion $\operatorname{erfc}(x) = 1 - \frac{2}{\sqrt{\pi}}\sum_{n=0}^{\infty}\frac{(-1)^n x^{2n+1}}{n!(2n+1)}$, Eq. (31) can be written as

$$ber_{\gamma_{FSO,th}} = \int_{\gamma_{FSO,th}}^{\infty}\left(1 - \frac{2}{\sqrt{\pi}}\sum_{n=0}^{\infty}\frac{(-1)^n \gamma^{(n+0.5)}}{n!(2n+1)}\right)\frac{1}{2\sqrt{32\pi\gamma}\sigma}\exp\left(\frac{-\left(\ln(\frac{\gamma}{\bar{\gamma}})+4\sigma^2\right)^2}{32\sigma^2}\right) \times\left(1 - \frac{2}{\sqrt{\pi}}\sum_{m=0}^{\infty}\frac{(-1)^m}{m!(2m+1)}\left(\frac{\ln(\frac{\gamma}{\bar{\gamma}})+4\sigma^2}{\sqrt{32}\sigma}\right)^{2m+1}\right) d\gamma \quad (32)$$

Applying change of variable $t = \frac{\ln(\gamma/\bar{\gamma})+4\sigma^2}{\sqrt{32}\sigma}$ Eq. (32) can be expressed as

$$ber_{\gamma_{FSO,th}} = I_1 - I_2 - I_3 + I_4 \quad (33)$$

where

$$I_1 = \frac{1}{2\sqrt{\pi}}\int_{\phi}^{\infty} e^{-t^2} dt \quad (34)$$

$$I_2 = \frac{1}{\pi}\sum_{n=0}^{\infty}\frac{(-1)^n \bar{\gamma}^{(n+0.5)} e^{-4\sigma^2(n+0.5)}}{n!(2n+1)}\int_{\phi}^{\infty} e^{-t^2+\sqrt{32}\sigma(n+0.5)t} dt \quad (35)$$

$$I_3 = \frac{1}{\pi}\sum_{m=0}^{\infty}\frac{(-1)^m}{m!(2m+1)}\int_{\phi}^{\infty} e^{-t^2} t^{2m+1}\mathrm{d}t \tag{36}$$

and

$$I_4 = \frac{2}{\pi^{3/2}}\sum_{n=0}^{\infty}\frac{(-1)^n\,\bar{\gamma}^{(n+0.5)} e^{-4\sigma^2(n+0.5)}}{n!(2n+1)}\sum_{m=0}^{\infty}\frac{(-1)^m}{m!(2m+1)}\int_{\phi}^{\infty} t^{(2m+1)} e^{-t^2+\sqrt{32}\sigma(n+0.5)t}\,\mathrm{d}t \tag{37}$$

where $\phi = \dfrac{\ln(\frac{\gamma_{FSO,th}}{\bar{\gamma}}) + 4\sigma^2}{\sqrt{32}\sigma}$. I_1 can be written in terms of the erfc function as

$$I_1 = \frac{1}{4} erfc(\phi) \tag{38}$$

I_2 can be calculated using Eq. (2.326) of [29] as

$$I_2 = \frac{1}{2\sqrt{\pi}}\sum_{n=0}^{\infty}\frac{(-1)^n\,\bar{\gamma}^{(n+0.5)} e^{4\sigma^2(2n^2+n)}}{n!(2n+1)}\,\mathrm{erfc}(\phi - \sqrt{8}\sigma(n+0.5)) \tag{39}$$

I_3 can be solved by using the exponential function's series form $e^x = \sum_{k=0}^{\infty}\frac{x^k}{k!}$ in Eq. (36); then

$$I_3 = \frac{1}{\pi}\sum_{m=0}^{\infty}\frac{(-1)^m}{m!(2m+1)}\left[\frac{\Gamma(m+1)}{2} - \sum_{k=0}^{\infty}\frac{(-1^k)}{k!}\left(\frac{\phi^{2m+2k+2}}{2m+2k+2}\right)\right] \tag{40}$$

where $\Gamma(t) = \int_0^{\infty} x^{t-1} e^{-x}\,\mathrm{d}x$ is the standard gamma function. Using Eq. (3.462) of [29], I_4 can be obtained as

$$I_4 = \frac{2}{\pi^{3/2}}\sum_{n=0}^{\infty}\frac{(-1)^n\,\bar{\gamma}^{(n+0.5)} e^{-4\sigma^2(n+0.5)}}{n!(2n+1)}\sum_{m=0}^{\infty}\frac{(-1)^m}{m!(2m+1)}\left\{2^{(-m-1)}\Gamma(2m+2)e^{4\sigma^2(n+0.5)^2}\right.$$
$$\left.\times D_{-2m+2}(-4\sigma(n+0.5)) - \left[\sum_{k=0}^{\infty}\frac{(-1)^k}{k!}\sum_{j=0}^{\infty}\frac{\left(\sqrt{32}\sigma(n+0.5)\right)^j}{j!}\left(\frac{\phi^{2m+2k+j+2}}{2m+2k+j+2}\right)\right]\right\} \tag{41}$$

where $D_v(q)$ is the parabolic cylinder function. For the RF link, using Eq. (19) in Eq. (30), $ber_{\gamma_{RF,th}}$ is given by

$$ber_{\gamma_{RF,th}} = \int_{\gamma_{RF,th}}^{\infty} 0.5\,\mathrm{erfc}\left(\sqrt{\gamma}\right)\frac{1}{\bar{\gamma}_{RF}} e^{\frac{-\gamma}{\bar{\gamma}_{RF}}}\,\mathrm{d}\gamma \tag{42}$$

Using the erfc function's series expansion and Eq. (3.351) of [29], $ber_{\gamma_{RF,th}}$ can be given as

$$ber_{\gamma_{RF,th}} = \frac{1}{2\bar{\gamma}_{RF}}\left\{\left(\bar{\gamma}_{RF} e^{\frac{-\gamma_{RF,th}}{\bar{\gamma}_{RF}}}\right) - \left(\frac{2}{\sqrt{\pi}}\sum_{k=0}^{\infty}\frac{(-1)^k}{k!(2k+1)} e^{\frac{-\gamma_{RF,th}}{\bar{\gamma}_{RF}}}\sum_{m=0}^{k+0.5}\frac{(k+0.5)!}{m!}\frac{\gamma_{RF,th}{}^m}{\bar{\gamma}_{RF}{}^{m-k-1.5}}\right)\right\} \tag{43}$$

4.3. Ergodic Capacity

The ergodic capacity of the considered system can be written as

$$C = C_{\gamma_{FSO,th}} + C_{\gamma_{RF,th}} F_{\gamma_{FSO}}(\gamma_{FSO,th}) \tag{44}$$

where $C_{\gamma_{FSO,th}}$ is the capacity contribution of the dual-hop FSO link, which is given by

$$C_{\gamma_{FSO,th}} = \int_{\gamma_{FSO,th}}^{\infty} B_{FSO}\log_2(1+\gamma) f_{\gamma_{FSO}}(\gamma)\mathrm{d}\gamma \tag{45}$$

and $C_{\gamma_{RF,th}}$ is the capacity contribution of the RF link, which is given by

$$C_{\gamma_{RF,th}} = \int_{\gamma_{RF,th}}^{\infty} B_{RF}\log_2(1+\gamma) f_{\gamma_{RF}}(\gamma)\mathrm{d}\gamma \tag{46}$$

where B_{FSO} is the bandwidth of the dual-hop FSO link, and B_{RF} is the bandwidth of the RF link. Using Eq. (25) in Eq. (45), and applying the well-known approximation $\ln(1+\gamma) \approx \ln(\gamma)$ [15], the capacity of the dual-hop FSO link $C_{\gamma_{FSO,th}}$ can be expressed for the symmetrical hops as

$$C_{\gamma_{FSO,th}} \approx \int_{\gamma_{FSO,th}}^{\infty}\frac{B_{FSO}}{\sqrt{32\pi}\gamma\sigma}\log_2(\gamma)\,\exp\left(\frac{-\left(\ln(\frac{\gamma}{\bar{\gamma}})+4\sigma^2\right)^2}{32\sigma^2}\right)\left(1 - \frac{2}{\sqrt{\pi}}\sum_{n=0}^{\infty}\frac{(-1)^n}{n!(2n+1)}\left(\frac{\ln(\frac{\gamma}{\bar{\gamma}})+4\sigma^2}{\sqrt{32}\sigma}\right)^{2n+1}\right)\mathrm{d}\gamma \tag{47}$$

Applying change of variable $t = \dfrac{\ln(\frac{\gamma}{\bar{\gamma}}) + 4\sigma^2}{\sqrt{32}\sigma}$ Eq. (47) can be expressed as

$$C_{\gamma_{FSO,th}} \approx J_1 - J_2 \tag{48}$$

where

$$J_1 = \frac{B_{FSO}}{\sqrt{\pi}}\int_{\phi}^{\infty}\log_2(\bar{\gamma} e^{(\sqrt{32}\sigma t - 4\sigma^2)}) e^{-t^2}\,\mathrm{d}t \tag{49}$$

and

$$J_2 = \frac{2B_{FSO}}{\pi}\int_{\phi}^{\infty}\log_2(\bar{\gamma} e^{(\sqrt{32}\sigma t - 4\sigma^2)}) e^{-t^2}\sum_{n=0}^{\infty}\frac{(-1)^n t^{2n+1}}{n!(2n+1)}\mathrm{d}t \tag{50}$$

Using the basic rules of logarithms in Eqs. (49) and (50), and using the exponential function's power-series representation in Eq. (50), J_1 and J_2 can be solved as

$$J_1 = a_1 erfc(\phi) + a_2 e^{-\phi^2} \tag{51}$$

and

$$J_2 = \frac{4a_1}{\pi}\sum_{n=0}^{\infty}\frac{(-1)^n}{n!(2n+1)}\left\{\frac{\Gamma(n+1)}{2}-\sum_{k=0}^{\infty}\frac{(-1)^k}{k!}\left(\frac{\phi^{2n+2k+2}}{2n+2k+2}\right)\right\}+\frac{4a_2}{\sqrt{\pi}}\sum_{n=0}^{\infty}\frac{(-1)^n}{n!(2n+1)} \times\left\{\frac{\Gamma\left(\frac{2n+3}{2}\right)}{2}-\sum_{k=0}^{\infty}\frac{(-1)^k}{k!}\left(\frac{\phi^{2n+2k+3}}{2n+2k+3}\right)\right\} \tag{52}$$

where $a_1 = \left[B_{FSO}(\log_2(\bar{\gamma}) - 4\sigma^2\log_2(e))\right]/2$, and $a_2 = B_{FSO}\sqrt{8/\pi}\,\sigma\log_2(e)$. For the RF link, using Eq. (19) in Eq. (46), the capacity of the RF link can be given by

$$C_{\gamma_{RF,th}} = \int_{\gamma_{RF,th}}^{\infty} B_{RF}\log_2(1+\gamma)\frac{1}{\bar{\gamma}_{RF}}e^{\frac{-\gamma}{\bar{\gamma}_{RF}}}\mathrm{d}\gamma \tag{53}$$

Using integration by parts and the approximation $\ln(1+\gamma) \approx \ln(\gamma)$, Eq. (53) can be expressed as

$$C_{\gamma_{RF,th}} = B_{RF}\left[\log_2(\gamma_{RF,th})e^{\frac{-\gamma_{RF,th}}{\bar{\gamma}_{RF}}} + \frac{1}{\ln(2)}E_1\left(\frac{\gamma_{RF,th}}{\bar{\gamma}_{RF}}\right)\right] \tag{54}$$

where $E_1(x) = \int_1^{\infty}\frac{e^{-xt}}{t}\mathrm{d}t$ is the exponential integral.

V. RESULTS AND DISCUSSION

In this section we provide numerical results for the outage probability, average BER, and ergodic capacity of the dual-hop FSO system with RF backup link. The performance is evaluated under clear, rainy, and foggy weather conditions. The performance of the considered system is compared to that of the FSO system without an RF backup link. Table 1 contains the FSO and RF channel parameters, which are extracted from [16], [28], [30], [31].

Figure 2 shows the outage probability of the dual-hop FSO system, with and without RF backup link, versus the transmitting power P_S, for various weather conditions. It can be observed that, at low values of P_S, the outage probability of the considered system in foggy weather is lower than that under rainy conditions. For example, at $P_S = -10$ dBm, the outage probability is on the order of 10^{-2} and 10^{-1} under conditions of fog and rain respectively. That is, due to the fact that at low P_S, with poor FSO link quality, the system relies mainly on the RF link, which is more affected by rain than fog. However, as P_S increases, the quality of the FSO links increases, and the system starts to rely more on the FSO links for transmission.

TABLE 1. Parameters of the FSO and RF links

	Symbol	Definition	Value
FSO links	λ	Wavelength	1550 nm
	L_i	FSO hop distance	1 km
	μ_S	Modulation index	1
	σ_i^2	Noise variance	$10^{-14}\,A^2$
	$\gamma_{FSO,th}$	Threshold SNR	10 dB
	P_R	Output power at R	P_S^2
RF link	fc	Carrier frequency	60 GHz
	L	Link distance	2 km
	G_t	Transmitter antenna gain	44 dBi
	G_r	Receiver antenna gain	44 dBi
	a_{oxy}	Oxygen attenuation	15.1 dB/km
	$\gamma_{RF,th}$	Threshold SNR	5 dB
	P_{RF}	Transmitting power	50 mW
	B_{RF}	Bandwidth	250 MHz
	N_0	Noise power spectral density	-114 dBm/MHz
	N_F	Receiver noise figure	5 dB

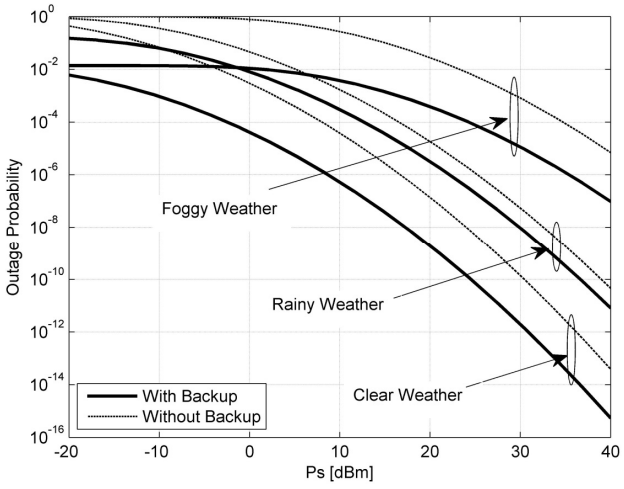

FIG. 2. The outage probability of the dual-hop FSO system with and without RF backup link versus the transmitted power P_S.

As can be seen from Fig. 2, at moderate values of P_S the performance becomes better in rainy weather. For example, at $P_S = 20$ dBm, the outage probability is on the order of 10^{-5} and 10^{-3} under conditions of rain and fog respectively. This is because fog is a major degrading factor for FSO links. In comparison to the dual-hop FSO system, the importance of using an RF backup link is obvious in clear and foggy weather, but not in rainy weather. In fact, at a target outage probability of 10^{-4}, a performance gain of 10 dB is achieved in clear and foggy weather, while in rainy weather around 3 dB of gain is observed.

Figure 3 shows the average BER of the considered system and the dual-hop FSO system against the transmitted power P_S, for various weather conditions. It can be seen that at low values of P_S the considered system provides better performance in foggy weather compared to rainy weather, while for higher values of P_S the performance becomes better in rainy weather. We can also observe that the average BER improves as P_S increases. Moreover, considerable performance gain is achieved when compared to the dual-hop FSO system. For example, at a target BER of 10^{-6}, the average BER is improved by 9 dB, 18 dB, and 19 dB in rainy, clear, and foggy weather, respectively. However, this gain decreases as the value of P_S increases, due to less dependence on the backup link.

Figure 4 shows the capacity of the considered system and the dual-hop FSO system versus the transmitting power P_S, for various weather conditions. It can be seen

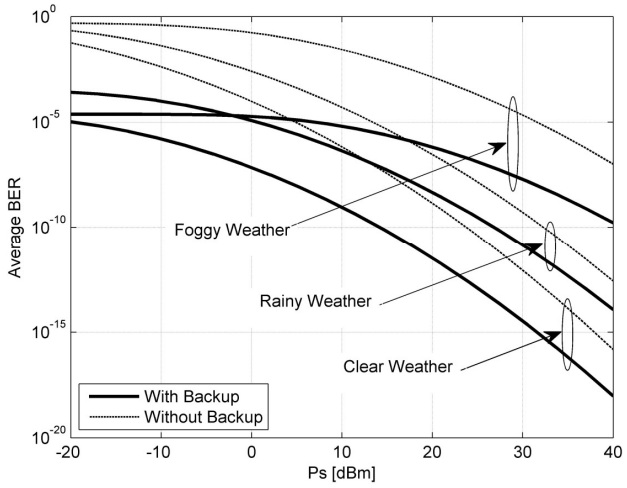

FIG. 3. The average BER of the dual-hop FSO system with and without RF backup link versus the transmitted power P_S.

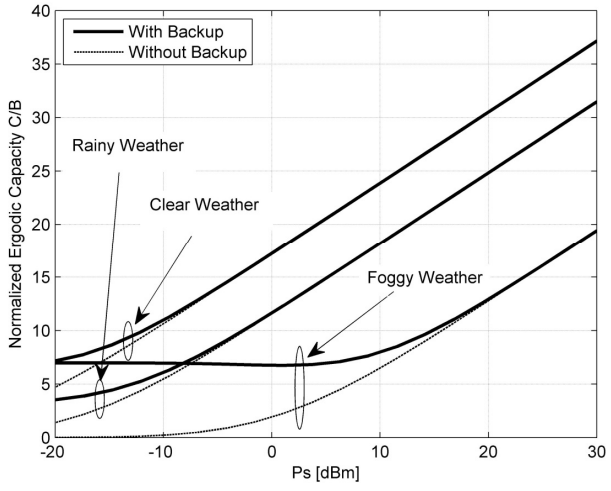

FIG. 4. The normalized ergodic capacity of the dualhop FSO system with and without RF backup link versus the transmitted power P_S.

that, for low values of P_S, the capacity of the considered system is better in foggy weather than in rain. However, at higher values of P_S, the performance becomes better in rainy weather. In addition, it can be observed from Fig. 4 that, at low and moderate values of P_S, the capacity under foggy conditions is limited to the capacity of the RF link. This is due to the lack of dependence on FSO links. We can also observe that the quality of the FSO links increases as P_S increases, and thus the overall capacity performance becomes better. In comparison to the dual-hop FSO system, it can be seen that the performance gain is mainly achieved in foggy weather, and decreases with increasing P_S. For example, when P_S increases from -10 dBm to 10 dBm, the performance gain is reduced by 71%. However, less improvement is achieved in clear and rainy weather. This is because under these conditions, as mentioned previously, the system is less dependent on the RF link than it is in foggy weather.

VI. CONCLUSION

In this work, a dual-hop FSO system with AF relaying protocol and an RF backup link was considered. Expressions for the CDF and the PDF of the end-to-end signal-to-noise ratio were obtained, and the performance of the considered system in terms of outage probability, average BER, and ergodic capacity under different weather conditions were derived. The results showed a significant performance gain, achieved by exploiting the RF backup link, especially at low and moderate FSO link quality. That gain is superior in foggy weather, as compared to clear and rainy conditions.

ACKNOWLEDGMENT

The authors would like to thank the Deanship of scientific research for funding and supporting this research, through the initiative of DSR Graduate Students Research Support (GSR).

REFERENCES

1. A. Malik and P. Singh, "Free space optics: current applications and future challenges," Int. J. Opt. **2015**, 1-7 (2015).
2. W. Lim, "BER analysis of coherent free space optical systems with BPSK over gamma-gamma channels," J. Opt. Soc. Korea **19**, 237-240 (2015).
3. X. Song, F. Yang, J. Cheng, N. Al-Dhahir, and Z. Xu, "Subcarrier phase shift keying systems with phase errors in lognormal turbulence channels," J. Lightwave Technol. **33**, 1896-1904 (2015).
4. L. Yang, X. Song, J. Cheng, and J. F. Holzman, "Free-space optical communications over lognormal fading channels using OOK with finite extinction ratios," IEEE Access **4**, 574-584 (2016).

5. G. Yang, Z. Li, M. Bi, X. Zhou, R. Zeng, T. Wang, and J. Li, "Channel modeling and performance analysis of modulating retroreflector FSO systems under weak turbulence conditions," IEEE Photonics J. **9**, 1-10 (2017).
6. L. Yang, B. Zhu, J. Cheng, and J. F. Holzman, "Free-space optical communications using on-off keying and source information transformation," J. Lightwave Technol. **34**, 2601-2609 (2016).
7. V. Khandelwal, R. Kaushik, and R. C. Jain, "A simple closed form approximation of average channel capacity for weakly turbulent optical wireless links," Wireless Pers. Commun. **95**, 2665-2677 (2017).
8. M. A. Esmail, H. Fathallah, and M.-S. Alouini, "On the performance of optical wireless links over random foggy channels," IEEE Access **5**, 2894-2903 (2017).
9. M. A. Kashani, M. M. Rad, M. Safari, and M. Uysal, "All-optical amplify-and-forward relaying system for atmospheric channels," IEEE Commun. Lett. **16**, 1684-1687 (2012).
10. P. Puri, P. Garg, and M. Aggarwal, "Analysis of spectrally efficient two way relay assisted free space optical systems in atmospheric turbulence with path loss," Int. J. Commun. Syst. **29**, 99-112 (2014).
11. J. Zhang, L. Dai, Y. Zhang, and Z. Wang, "Unified performance analysis of mixed radio frequency/free-space optical dual-hop transmission systems," J. Lightwave Technol. **33**, 2286-2293 (2015).
12. P. V. Trinh, T. C. Thang, and A. T. Pham, "Mixed mmWave RF/FSO relaying systems over generalized fading channels with pointing errors," IEEE Photonics J. **9**, 1-14 (2017).
13. A. M. Salhab, "A new scenario of triple-hop mixed RF/FSO/RF relay network with generalized order user scheduling and power allocation," EURASIP J. Wireless Commun. Networking **2016**, 260 (2016).
14. M. Usman, H. C. Yang, and M. S. Alouini, "Performance analysis of switching based hybrid FSO/RF transmission," in *Proc. IEEE 80th Vehicular Technology Conference (VTC2014-Fall)* (Canada, Sept. 2014), pp. 1-5.
15. M. Usman, H. C. Yang, and M. S. Alouini, "Practical switching-based hybrid FSO/RF transmission and its performance analysis," IEEE Photonics J. **6**, 1-13 (2014).
16. N. D. Chatzidiamantis, G. K. Karagiannidis, E. E. Kriezis, and M. Matthaiou, "Diversity combining in hybrid RF/FSO systems with PSK modulation," in *Proc. IEEE International Conference on Communications (ICC)* (Japan, Jun. 2011), pp. 1-6.
17. T. Rakia, H. C. Yang, M. S. Alouini, and F. Gebali, "Outage analysis of practical FSO/RF hybrid system with adaptive combining," IEEE Commun. Lett. **19**, 1366-1369 (2015).
18. H. Kazemi, M. Uysal, F. Touati, and H. Haas, "Outage performance of multihop hybrid FSO/RF communication systems," in *Proc. 4th International Workshop on Optical Wireless Communications (IWOW)* (Turkey, Sept. 2015), pp. 83-87.
19. X. Song and J. Cheng, "Optical communication using subcarrier intensity modulation in strong atmospheric turbulence," J. Lightwave Technol. **30**, 3484-3493 (2012).
20. K. Prabu, S. Cheepalli, and D. S. Kumar, "Analysis of PolSK based FSO system using wavelength and time diversity over strong atmospheric turbulence with pointing errors," Opt. Commun. **324**, 318-323 (2014).
21. M. R. Handura, K. M. Ndjavera, C. N. Nyirenda, and T. O. Olwal, "Determining the feasibility of free space optical communication in Namibia," Opt. Commun. **366**, 425-430 (2016).
22. A. Vavoulas, H. G. Sandalidis, and D. Varoutas, "Weather effects on FSO network connectivity," J. Opt. Commun. Networking **4**, 734-740 (2012).
23. T. H. Carbonneau and D. R. Wisely, "Opportunities and challenges for optical wireless: the competitive advantage of free space telecommunications links in today's crowded marketplace," Proc. SPIE **3232**, 119-128 (1998).
24. M. Abaza, R. Mesleh, A. Mansour, and E.-H. Aggoune, "Performance analysis of miso multi-hop FSO links over log-normal channels with fog and beam divergence attenuations," Opt. Commun. **334**, 247-252 (2015).
25. S. M. Navidpour, M. Uysal, and M. Kavehrad, "BER performance of free-space optical transmission with spatial diversity," IEEE Trans. Wireless Commun. **6**, 2813-2819 (2007).
26. E. S. Altubaishi and X. Shen, "Performance analysis of spectrally efficient amplify-and-forward opportunistic relaying scheme for adaptive cooperative wireless systems," Wireless Commun. Mobile Computing **15**, 1247-1258 (2015).
27. M. K. Simon and M. S. Alouini, *Digital communication over fading channels* (John Wiley & Sons, New Jersey, USA, 2005).
28. J. Zhao, S. Zhao, W. Zhao, and K. Chen, "Performance analysis for mixed FSO/RF Nakagami-*m* and Exponentiated Weibull dual-hop airborne systems," Opt. Commun. **392**, 294-299 (2017).
29. I. S. Gradshteyn and I. M. Ryzhik, *Table of integrals, series, and products* (Academic Press, 2014).
30. I. Recommendation, "838-3. specific attenuation model for rain for use in prediction methods," ITU-R Recommendations, P Series Fasicle, ITU, Geneva, Switzerland (2005).
31. B. He and R. Schober, "Bit-interleaved coded modulation for hybrid RF/FSO systems," IEEE Trans. Commun. **57**, 3753-3763 (2009).